AUTOMATIC DETECTION OF DETACHED AND ERRONEOUS ELECTRODES IN ELECTRICAL IMPEDANCE TOMOGRAPHY

Yednek Asfaw, Andy Adler

School of Information and Technology, University of Ottawa, Ottawa, Canada;
{yasfaw,adler}@site.uottawa.ca

ABSTRACT: One unfortunate occurrence in experimental measurements with electrical impedance tomography is electrodes which become detached or poorly connected, such that the measured data cannot be used. This paper presents an automatic approach to detect such erroneous electrodes. It is based on the assumption that all valid measurements are related by the image reconstruction model, while the measurements from erroneous electrodes are unrelated. The method calculates an estimate of the data at an electrode, based on the measurements from all other electrodes, and compares this to the measurements. If these data match, the set of electrodes does not contain an erroneous electrode. In order to detect an erroneous electrode amongst *N* electrodes, all sets of *N-1* electrodes are tested, and the set with the best match between measurements and estimate is identified as the one which excludes the erroneous electrode. Tests were performed on experimental data and showed consistent identification of erroneous electrodes with those made by a trained user.

Keywords: Electrical Impedance Tomography, Electrode Errors, Image Reconstruction

1. INTRODUCTION

Electrical Impedance Tomography (EIT) uses body surface electrodes to make measurements from which an image of the conductivity distribution is calculated. However, one important difficulty with experimental and clinical EIT measurements is the care required to ensure proper electrode measurements. Many conditions can cause electrodes to give false readings, such as electronics noise and errors [3], as well as poor electrode contact due to patient movement [5], sweat and peripheral oedema, especially in long term monitoring applications [6]. Given a set of data containing measurements with errors, it is desired to calculate an image based on the remaining good data. In order to accomplish this, we have developed a methodology to reconstruct EIT images in the presence of single electrode errors [2].

One limitation of our previous work is the requirement that the erroneous electrodes must be identified to the algorithm by an operator. However, the ability to automatically identify erroneous electrodes is a potentially important capability for clinical and experimental applications of EIT. In this paper, we present a method to allow automatic detection of such erroneous electrodes.

2. METHODS AND DATA

The presence of an erroneous electrode in EIT introduces artefacts into the reconstructed images. This suggests a test for the presence of faulty electrodes could be based on analysis of images for unusual features. The disadvantage of such an heuristic approach is the difficulty in defining the nature of such an image artefact, in relation to an unusual, but accurate, measurement.

We propose a method based on comparing the measurements obtained on all electrodes to each other. Since all electrodes measure the same medium, it is reasonable to expect that “good” electrodes will produce measurements consistent with each other. The “consistency” of a set of electrodes can be verified by estimating the measured data at each electrode in the set, using only measurements on other electrodes ([2]), and then comparing the estimate to the actual data measured. A set of electrodes with consistent measurements must contain all "good" electrodes. In order to test an *N* electrode EIT system, we test all possible sets of *N-1* electrodes; if only one of the subsets contains all "good" electrodes, then the electrode excluded from that set must be erroneous.

2.1. Image reconstruction with missing data

We consider EIT difference imaging. The forward model estimates the vector of the change in conductivity distribution (**x**) from a vector of change in difference measurements (**z**) and Gaussian noise (**n**). For small changes in **x**, the relationship is linearized as:

$$\mathbf{z} = \mathbf{H}\mathbf{x} + \mathbf{n} \tag{1}$$

where **H** is the Jacobian (sensitivity). The EIT image reconstruction algorithm will then calculate an estimate of the change in conductivity ($\hat{\mathbf{x}}$) from **z**. For a one pass algorithm [2], image reconstruction may be simplified to a single matrix multiplication, expressed as:

$$\hat{\mathbf{x}} = \mathbf{B}\mathbf{z} \tag{2}$$

It is possible to modify **B** to estimate ($\hat{\mathbf{x}}$) using a subset of the available measurements. One approach [2] is to express image reconstruction in terms of MAP regularization, and set the noise variance on unused measurements to ∞. We use the notation $\mathbf{B}(e_i, e_j)$ for the reconstruction matrix designed not to use measurements made with electrodes e_i and e_j.

2.2 Detection of erroneous electrodes

The following method analyses difference EIT data from a set of electrodes *S*, in order to detect the presence of a single erroneous electrode. Figure 1 outlines the steps of the method.

Define set S = { e_i | i = 1....N}
For all e_i in S
  Define set, S′, without electrode e_i: S′= { e_j : j = 1....N, j≠i}
  For all e_j in S′
    Calculate image: $\hat{\mathbf{x}} = \mathbf{B}(e_i, e_j)\mathbf{z}$
    Estimate measurements on e_j: $\hat{\mathbf{z}}_j = \mathbf{H}_j\hat{\mathbf{x}}$
    Calculate: $E_j = \|\mathbf{z}_j - \hat{\mathbf{z}}_j\|$
  $T_i = \sum_{j=1, j\neq i}^{N} E_j$
If T_i is significantly less than other values, **detect** e_i as erroneous electrode

Figure 1: Pseudocode for detection of an erroneous electrode.

We iterate over each electrode e_i in S, forming a set S′ of all electrodes not including e_i. S′ is then tested to calculate a parameter T_i which reflects the consistency of measurements among electrodes in S′. If T_i is low, S′ contains all "good" electrodes, otherwise it contains at least one erroneous electrode. T_i is the sum of estimation errors E_j for each electrode e_j in S′. The estimation error is defined as:

$$E_j = \|\mathbf{z}_j - \hat{\mathbf{z}}_j\| \tag{3}$$

where $\mathbf{z}_j$ is the vector of differential measurements made using e_j, and $\hat{\mathbf{z}}_j$ is the estimate of $\mathbf{z}_j$ based on all electrodes in S′ except e_j. It is calculated by

$$\hat{\mathbf{z}}_j = \mathbf{H}_j\hat{\mathbf{x}} \tag{4}$$

where $\mathbf{H}_j$ is the rows of the sensitivity matrix $\mathbf{H}$ which correspond to measurements on e_j, and

$$\hat{\mathbf{x}} = \mathbf{B}(e_i, e_j)\mathbf{z} \tag{5}$$

It is necessary to calculate the estimate without measurements from electrodes e_i and e_j, because e_i is not part of S′, and e_j is the electrode is being estimated. After T_i values are calculated, they are tested against each other to detect if any are significantly less than the others. If T_i meets this condition, electrode e_i is detected as an erroneous electrode.

2.3 Data

EIT data were obtained from previous experiments [3]. Mechanically ventilated mongrel dogs had sixteen ECG-style electrodes spaced evenly around the shaved thorax 10 cm above the base of the rib cage. Data acquisition was triggered 100 ms after the QRS peak of the ECG at end expiration and end inspiration. Adjacent drive EIT measurements were acquired every half hour for six hours. Four animals, of nineteen, showed some level of electrode errors. Images were calculated corresponding to data measured at each inspiration. The gold standard for electrode error was based on human assessment. A graphic user interface was designed to present reconstructed EIT images to experienced users. Users were asked to classify each image as either: 1) No error, 2) Possible error, or 3) Error (definite).

3 RESULTS

This method was applied to the three sets of representative EIT data: data with no error (Fig. 2A), data with a small error (Fig. 2B), and data with a typical error (Fig. 2C) (based on our experience of EIT errors). The reconstructed images and graphs of T_i vs. electrode number are shown. Data with errors (2B and 2C) show higher overall values of T_i, compared to error free data (2A). In both cases, electrodes with errors have significantly lower T_i ($p<0.05$), although the significance level is greater with larger error (2C). Data with large errors is not presented, but tests also show significantly lower T_i for erroneous electrodes. In the case of Fig. 2C, two adjacent electrodes are detected. We have noted that this is not uncommon result with this method with larger data errors. The method is currently implemented in Matlab, and requires 20 sec. for each EIT data set on an Athlon 1.8Ghz computer.

4 DISCUSSION

In this paper, we have presented a method to automatically detect an erroneous electrode in EIT data. The method is based on the assumption that an erroneous electrode produces measurements inconsistent with those from other good electrodes. Results show that the method is able to correctly detect the presence of and identify the location of erroneous electrodes in sample data. Currently, the detection threshold was set to the minimum level, allowing the method to prefer false identification of errors. One possible extension to the method is for detection of multiple electrode errors by selecting two or more candidate electrodes at a time.

Automatic detection of electrode errors in EIT has several possible applications. In offline processing, such a technique could identify and correct for such errors. More usefully, if implemented in EIT monitoring equipment, it would be possible to alert staff who could then attend to the problem. However, for such online applications, the algorithm is still too slow (30s) for real-time data analysis, but would permit erroneous error detection in the background.

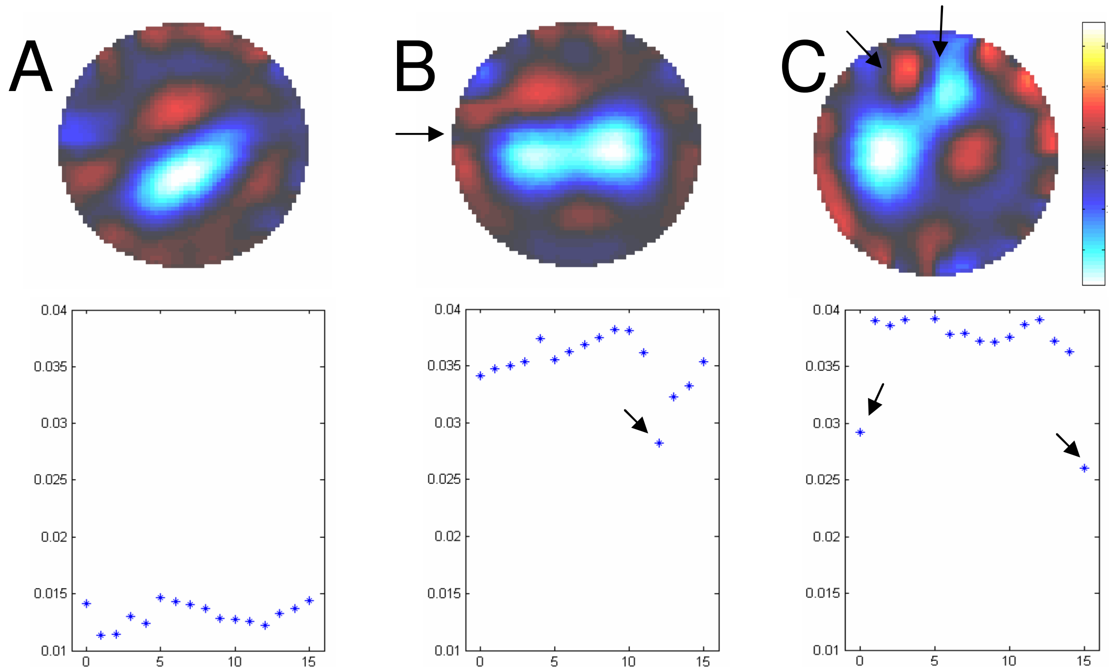

Figure 2: *Upper row*: images of tidal ventilation in a dog. Electrodes are numbered clockwise with electrode zero at the top centre. Images are individually normalized to the colourscale (arbitrary units) at right. *Bottom row*: parameter T for each electrode. (A) no erroneous electrode (B) data with erroneous electrode with small error signal (C) data with erroneous electrode with typical error signal. Arrows show the location of the erroneous electrode(s).

ACKNOWLEDGEMENT

We would like to thank Richard Bayford for providing experimental data and encouragement in this work.

REFERENCES

1. Adler A, Guardo R, Electrical Impedance Tomography: Regularised imaging and Contrast Detection, *IEEE Trans. Medical Imag.*, **15** 170-179, 1996.
2. Adler A, Accounting for erroneous electrode data in Electrical Impedance Tomography, *Physiol. Meas.*, **25** 227-238, 2004.
3. Adler A, Amyot R, Guardo R, Bates J H T, Berthiaume Y, Monitoring changes in lung air and liquid volumes with electrical impedance tomography, *J. Appl. Physiol.,* **83** 1762-1767, 1997.
4. Al-Hatib F, Patient-instrument connection errors in bioelectrical impedance measurement, *Physiol. Meas.*, **19** 285-296, 1998.
5. Blott B H, Daniell G J, Meeson S, Electrical impedance tomography with compensation for electrode postitioning variations, *Phys. Med. Biol.,* **43** 1731-1739, 1998.
6. Lozano A, Rosell J, Pallás-Areny R, Errors in prolonged electrical impedance measurements due to electrode repositioning and postural changes, *Physiol. Meas.*, **16** 121-130, 1995.